Effect of Artificial Roughness Geometries on Thermo-Hydraulic Efficiency of Solar Air Heater

Surendra Agrawal [1], J.L. Bhagoria[2]
[1]*Deparment of Mechanical Engineering, Surabhi & Satyam Group, Bhopal (MP), India*
[2]*Deparment of Mechanical Engineering, M.A.N.I.T., Bhopal (MP), India*
bitsurendra@gmail.com, palak_bh@rediffmail.com

Abstract: In order to make the solar air heater economically more viable, their thermal efficiency needs to be improved. This can be done by enhancing the heat transfer co-efficient between the absorber plate and air flow through a duct. In general, heat transfer enhancement techniques are divided into two groups: active & passive techniques. Providing an artificial roughness on a heat transferring surface is an effective passive heat transfer technique to enhance the rate of heat transfer to fluid flow. In this paper, reviews of various artificial roughness elements used as passive heat transfer techniques, in order to improve thermo hydraulic performance of a solar air heater, is done. The objective of this paper is to review various studies, in which different artificial roughness elements are used to enhance the heat transfer rate with little penalty of friction. The effects of various rib parameters on heat transfer and fluid flow processes are also discussed.

Keywords:*Artificial roughness geometries, Thermo-hydraulic performance, solar air heater, heat transfer co-efficient, friction factor, Reynolds number, etc.*

*****

1. INTRODUCTION

Due to limited conventional energy resources an alternative finding is necessary, as energy in various forms has been playing an important role to sustain fast economic and industrial growth worldwide. Of many alternatives, solar energy stands out as brightest long range resource for meeting continuously increasing demand for energy [1]. It is considered to be a dominating renewable energy source due to its large potential, free availability and non-polluting behaviour with a minimum of adverse environmental risks. Though it is location and time dependent and requires efficient collection and storage systems for economical utilization. The simplest method to utilize solar energy for heating applications is solar collectors [2]. These solar air heaters absorb the irradiance and convert it into thermal energy at the absorbing surface and then transfer this energy to the air flowing through it.

Solar air heaters form the foremost component of solar energy utilization system because of minimal use of materials cost and also due to their inherent simplicity. But the main demerit of solar air heater is less thermal efficiency because of low rate of heat transfer capability between absorber plate and air flowing in the duct. This is because of the formation of laminar viscous sub layer which resist the heat transfer. There are various Active & passive methods to increase heat transfer coefficients. The active techniques require external forces, e.g. electric field and surface vibration. The passive techniques require special surface geometries, such as rough and external surface, fluid additives and swirl flow devices i.e. twisted tap inserts to create a swirling flow. The attempts adopted to enhance the heat transfer includes provision of artificial roughness as a passive techniques on the underside of absorber plate in the form of ribs, grooves/dimples, baffles, mesh wires, etc used by various researchers. In this paper, reviews of various artificial roughness elements used as passive heat transfer techniques, in order to improve thermo hydraulic performance of a solar air heater, is done. The objective of the present paper is

(1) To review the research of different investigators in terms of roughness geometries, which can enhance convective heat transfer in solar air heaters with minimum increase in friction losses [3].

(2) To classify various types of roughness geometries so that for a specific purpose particular type of geometry can be selected as per the need.

(3) To discuss various types of roughness geometry in terms of geometrical and operating parameters.

(4) To discuss the variation of Nusselt number & friction factor dependence with respect to geometrical and operating parameters.

Nomenclature

A_s	Absorber plate area, m^2	B/S	Relative roughness length ratio, i.e. segment length.
C_p	Specific heat of air at constant pressure, KJ/kg K	D_h	Equivalent diameter of air passage= 4WH/ [2(W+H)]
d/w	Relative gap position	d/D	Relative print diameter
e	Roughness height, mm	e+	Roughness Reynolds number
e/ D_h	Relative roughness height	e/d	Height to print diameter of protrusion
f	Friction factor	F_R	Collector heat removal factor
g	groove position, m	g/p	Relative groove position
G_d/L_v	relative gap distance	H	Height of air channel, m
h	Convective heat transfer coefficient,	I	Heat Flux, W *I* m^2
k	Thermal conductivity of air, W/m- °c	L	Length of test section of duct or longway length of mesh, m
l/s	relative length of metal grit	L/e	Relative long way length
m	Mass flow rate of air, kg/s	Nu	Nusselt number
p	Pitch	p/e	Relative roughness pitch
P'/P	Staggering ratio	□ P	Pressure drop across duct, Pa
Qa	Rate of heat transfer to air, W	Qu	Useful Rate of heat transfer to air, W
Q_L	heat loss ,W	Re	Reynolds number
S	Length of main segment line of discrete	S'	Length of staggered discrete rib element,
	rib element or shortway length, m	S'/S	Segment ratio
S/e	relative shortway length	T_{pm}	Mean plate temperature, K
Ta	Ambient temperature, K	T_{fm}	Average temperature of air, K
T_i	Inlet temperature of air, °c	T_o	Outlet temperature of air, °c
U_L	Overall loss coefficient, W/m2-K	V	Velocity of air, m/s
W	Width of air duct, m	W/H	Channel aspect ratio
W/w	relative width		

Greek Symbols

□$_{th}$Thermal efficiency□ Density of air, kg/m3

□ Dynamic Viscosity, Kg/m-secν Kinematic Viscosity, m2/ sec

α Angle of Attackδ Thickness of laminar sub layer

ϕ Rib chamfer/wedge angle τα Transmissivity–absorptivity product

Subscripts

s	Smooth channel	i	Inlet
o	Outlet	r	Rough channel

2. Concept & Methodology of Artificial Roughness

Artificial roughness is a passive heat transfer enhancement technique by which thermo hydraulic performance of a solar heater can be improved. When air flows over a heated surface, a thin layer called sub layer exists beneath the core turbulent flow region in which the flow remains predominantly laminar due to supremacy of viscous effects. The existence of a laminar sub-layer between the absorber plate and the flowing air is the main cause of high thermal resistance for heat. In order to attain higher heat transfer coefficient, it is enviable that flow at the heat transferring surface is made turbulent.Artificially roughened absorber plate is considered to be a good methodology to increase the heat transfer coefficient since it break laminar sub layer in order to reduce thermal resistance. But this also causes simultaneous increase in friction loss in duct. It is therefore desirable to create turbulence in the region very close to the heat transferring surface i.e.in the laminar sub layer only.This can be done

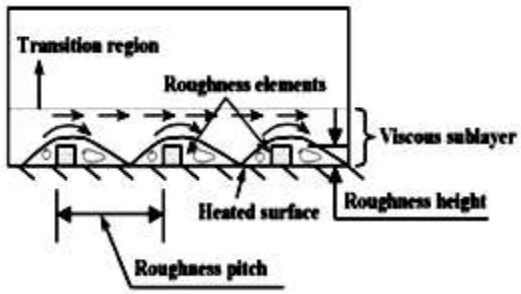

Fig. 1. Effects of roughness elements on flow field

by keeping the height of the roughness elements to be small in comparison with the duct dimension. Pressure drop could also be minimized to keep the height of the roughness element small. In order to select height of the artificial roughness element, it becomes imperative to know the thickness of the laminar sub layer[4].

The primary mechanisms for thinning the boundary layer are increased free stream velocity & turbulent mixing. Artificial roughness, provided on the underside of the absorber plate, creates local wall turbulence. Artificial geometry creates turbulence in the laminar sub layer due to flow separation and reattachment between the two repeated ribs, which enhances the heat transfer rate between the absorber plate and the flowing air of a solar air heater. Recirculation flow further enhances the convective heat transfer. Flow from the core to surface depletes the thickness of the boundary layer and the secondary flow from the surface to the core promotes mixing. **Fig.1** shows the flow pattern in the viscous sub layer region due to presence of repeated roughness elements [5].

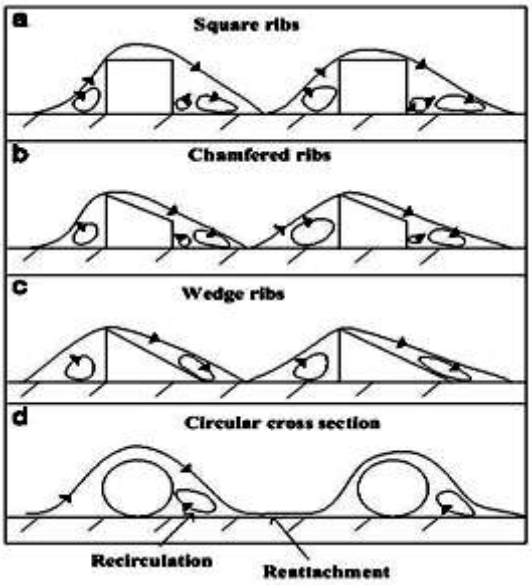

Fig. 2. Flow separation and vorticesformation

3. Roughness Parameters

In solar air heaters, artificial roughness in the form of attaching the small diameter wires, machining ribs of different shapes, forming dimples/protrusion have been investigated for performance enhancement of solar air heater as well as baffles are also used. There are many parameters that characterize the arrangement and shape of the roughness

elements; height (e) and pitch (p) of roughness element are the most important parameters. These are specified in non-dimensional form as relative roughness height (e/D_h) and relative roughness pitch (p/e) respectively. The other parameters include Reynolds number, rib cross-section, angle of attack, chamfering and combined turbulence promoters. The roughness elements can be two-dimensional ribs or three dimensional discrete elements, angled ribs, V-shaped continuous or broken ribs, rib-groove, arc rib, Multi v-rib, dimple or cavity or compound rib-grooved etc. Although circular ribs are the most commonly used geometry, square ribs, chamfered, baffles and grooved sections have also been investigated in order to find out most efficient arrangement for solar thermal energy utilization system. The key geometrical parameters that are used to characterize roughness are

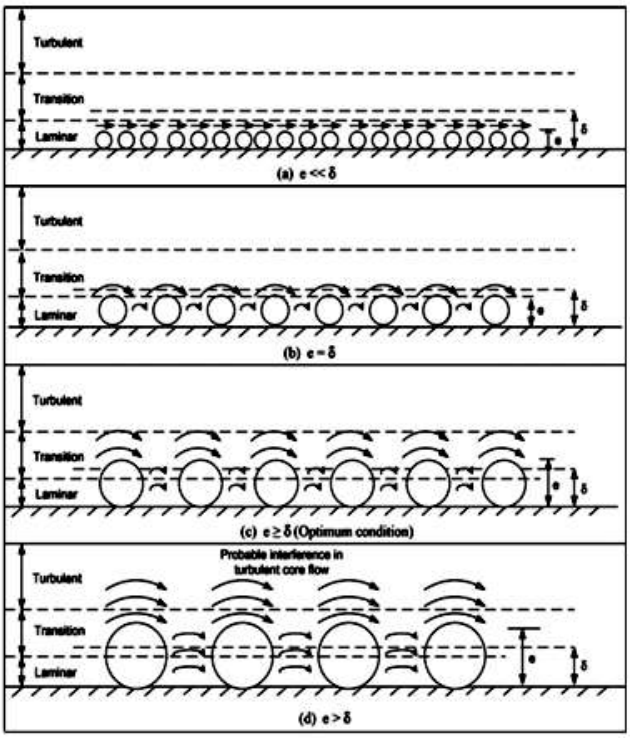

Fig. 3. Effect of rib height on laminar sub layer

3.1. Relative roughness height (e/D_h):- It is the ratio of rib height (e) to equivalent diameter (D_h) of air passage

3.2. Relative roughness pitch (p/e):- It is the ratio of distance between two consecutive ribs (p) & rib height (e).

3.3. Angle of attack (α):- It is the inclination of the rib with the direction of air flow in the duct.

3.4. Aspect ratio (W/H):- It is the ratio of duct width (W) to duct height (H).

4. Effects of rib & other parameters on flow patterns, heat transfer co-efficient & friction factor

4.1. Effect of rib & rib height

Actually the rib on the absorber plate creates two flow separation regions, one on each side of the rib. Separation creates vortices which lead to the generation of turbulence & hence the enhancement in heat transfer as well as friction losses takes place. For some types of ribs, the flow separation, free shears layer formation & vortices formation is shown in Fig.2. The rib height is approximately 15% of the plate separation distance for reducing friction losses [6].

4.2. Effect of Relative roughness height (e/D_h)

Fig.3 shows the effect of rib height on laminar sub layer explained by Prasad et al. [7]. They reported that,

(1) If **$e << \delta$**, roughness has no effect.

(2) If $e >> \delta$, roughness has more effect on fluid pressure as compared to heat transfer, due to probable interference of turbulence induced in the already turbulent core.

(3) If $e \geq \delta$, heat transfer has more effect with moderate effect on fluid pressure.

Prasad and Saini [8] show the flow pattern as a function of relative ribs height as shown in Fig. 4.They collected the data for Nusselt number and frictional factor & plotted then for different relative roughness height as a function of the Reynolds number as shown in Fig.5. Nusselt number and friction factor both increases with increase of relative roughness height. But the rate of increase of the average friction factor increases whereas the rate of increase of the average Nusselt number decreases with the increase of the relative roughness height. At very low Reynolds number the effect of e/D_h is insignificant on enhancement of Nusselt number. The maximum rib height should be such that the fin and flow passage blockage effects are negligible. Values of e/Dh has been shown in Table 1 for maximum value of heat transfer coefficients.

4.3. Effect of Relative roughness pitch (p/e)

Fig.6 shows the flow pattern of ribs of different relative roughness pitches. For a high heat transfer from absorber plates, the relative roughness pitch should be between 8 and 10. Due to separation at the rib, reattachment of the free shear layer does not occur for a relative roughness pitch (p/e) less than about 8 to 10, which results in the decrease of heat transfer rate. The rate of increase in friction factor will increase with the decrease of pitch. For relative roughness pitch (p/e) value of about 10 the reattachment point is reached and a boundary layer begins to grow before the succeeding rib is encountered. The local heat transfer coefficients in the separated flow region are larger than those of an undisturbed boundary layer and wall shear stress is zero at the reattachment point. The maximum heat transfer coefficient occurs in the vicinity of the reattachment point. A reverse flow boundary layer originates at the reattachment point and tends toward redevelopment downstream from the reattachment point. However, an increase in the relative

roughness pitch (p/e) beyond 10 resulted in the decrease of heat transfer enhancement. Nusselt number and frictional factor both increase with relative roughness pitch for constant relative roughness height as shown in Fig.7. Values of relative roughness pitch have been presented in Table 1 for maximum value of heat transfer coefficient.

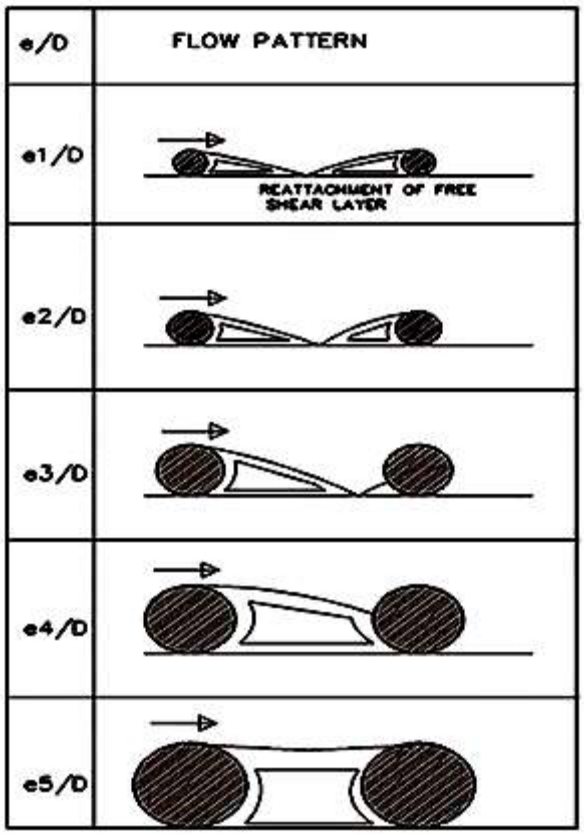

Fig. 4. Effect of e/D_h on flow pattern

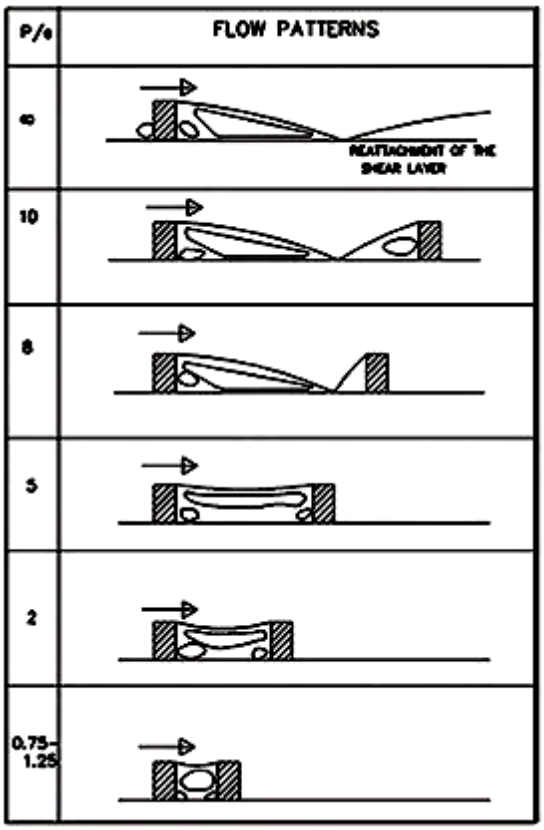

Fig. 6. Effect of p/e on flow pattern

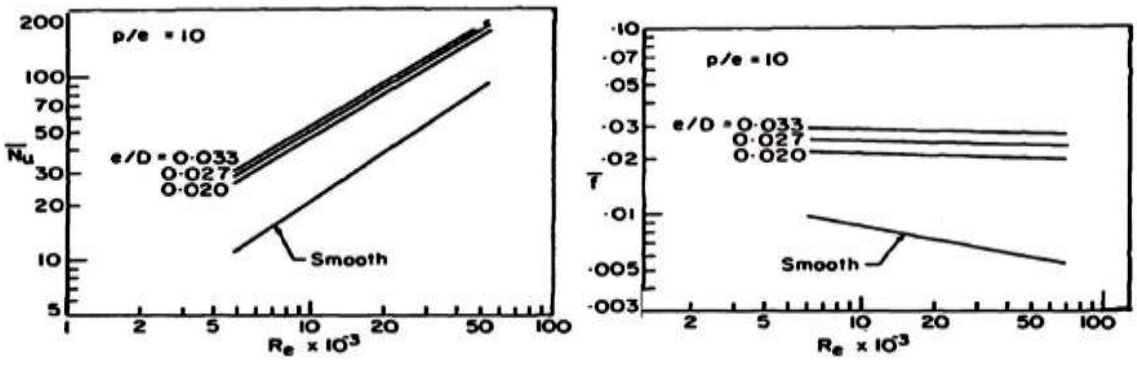

Fig. 5. Effect of relative roughness height on

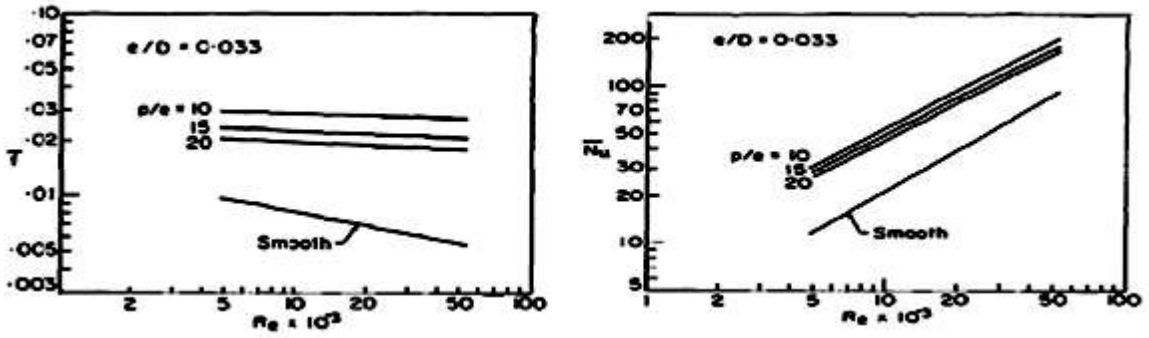

Fig.7. Effect of relative roughness pitch on Nusselt

Table 1 Values of (e/D_h) & (p/e) for maximum value of heat transfer rate for different artificial roughness geometries

S.N	Investigators	Roughness geometry	Value of (e/D_h)	Value of (p/e)	Angle of attack(α)
1	Prasad and Saini[7,8]	Transverse ribs	**0.0333**	**10**	
2	Momin et.al. [31]	V-shaped continuous ribs	**0.034**	**10**	**60^0**
3	Hans et al.[35]	Multi V-ribs	**0.043**	**8**	**60^0**
4	Aharwal et al.[28]	Inclined continuous ribs with gap	**0.0377**	**10**	**60^0**
5	Sukhmeet et al.[33]	Dis		**8**	**60^0**
6	Kumar et al.[11,55]	Multi V-shaped ribs with gap	**0.043**	**10**	**60^0**
7	Kumar et al.[39]	W-shaped discrete ribs	**0.0338**	**10**	**60^0**
8	Karmare & Tikekarv[49]	Metal grit rib roughness	**0.044**	**17.5**	
9	Layek et.ala.[46]	Transverse chamfered rib grooved	**0.04**	**10**	
10	Varun et al.[30]	Combination of inclined & transverse ribs	**0.03**	**8**	
11	Saini & Saini [40]	Arc shaped wire	**0.0422**	**10**	**α/90=0.333**
12	Saini & Verma [50]	Dimple shape roughness	**0.0379**	**10**	
13	Jaurker et.al. [45]	Transverse rib-grooved	**0.036**	**4.5-10**	
14	Bhagoria et.al.[48]	Transverse wedge	**0.033**	**7.57**	
15	Lanjewar et al.[36]	W-shaped ribs	**0.03375**	**10**	**60^0**
16	Karwa et al. [14]	Chamfered rib	**0.0328**	**7.09**	

4.4. Effect of inclination of rib (angle of attack)

Apart from the effect of rib height and pitch, the parameter that has been found to be most influential is the angle of attack of the flow with respect to the rib position i.e. skewness of rib towards the flow. Span wise counter rotating secondary flows created by angling of the rib; appear to be responsible for the significant span wise variation of heat transfer coefficient. It is pointed out that whereas the two fluid vortices immediately upstream and downstream of a transverse rib are essentially stagnant relative to the mainstream flow which raises the local fluid temperature in the vortices and wall temperature near the rib resulting in low heat transfer. The vortices in the case of angled ribs move along the rib so subsequently join the main stream, the fluid entering near the leading end of rib and coming out near the trailing end [9]. These moving vortices therefore bring in cooler channel fluid in contact with leading end raising heat transfer rate while the trailing end heat transfer is relatively lower as in Fig. 8 & 9. This phenomenon therefore results in strong span wise variation of heat transfer. The value of angle

of attack presented in Table 1 for the maximum value of heat transfer coefficient.

4.5. Effect of Position of gap in continuous ribs

With the introduction of a gap in a rib, secondary flow along the rib joins the main flow to accelerate it, which in turn, energizes the retarded boundary layer flow along the surface resulting in enhancement of heat transfer. Position of gap with respect to leading and trailing edge has a considerable effect on heat transfer enhancement. Position of the gap near the trailing edge, results in more contribution of secondary flow in energizing the main flow through the gap and recirculation loop in the remaining part of the rib, thereby, increasing the heat transfer rate[10] as in Fig.10

4.6. Effect of V-shaped ribs

V-shaped ribs further enhance the heat transfer rate as V-shaped ribs create two leading ends (region of high heat transfer rate) and a single trailing end (region of low heat transfer rate). The V-shaped rib creates two secondary flow vortices along the two angled ribs of the V-shaped ribs as compared to single secondary flow vortices of angled ribs as shown in Fig.11.V-shaped rib with apex facing downstream has a higher heat transfer as compared to that of with apex facing upstream [09]. Again multiple v-ribs increase heat transfer further on account of formation of higher number of leading ends and secondary flow cells [11]. According to researchers, there is a formation of two leading ends (where heat transfer rate is high) and a single trailing end (where heat transfer rate is low) as well as two secondary flow cells which promote turbulence mixing which causes increase in heat transfer.

4.7. Effect of Staggering in discrete v-shaped ribs

The v-shaped ribs along with staggered rib pieces in between further increase the number and area of heat transfer regions. Additional rib parameters related to the size and positioning of rib pieces (length ratio, B/S, segment ratio, S'/S and staggering ratio, P'/P) with respect to main rib produce complex interaction of secondary flow [12].

4.8. Effect of Chamfering of the rib

Chamfering of the rib decreases the reattachment length by deflecting the flow and to reattach it nearer to the rib. The decrease in reattachment length permits to organize the ribs more closely. Chamfering of the rib also increases the shedding of vortices generated at the rib top that results in increase turbulence. The optimum chamfering angle on the basis of thermo- dynamically performance has been reported equal to 15-18. For higher chamfer angle flow separates from the rib top surface & generates boundary layer, which decreases the heat transfer. The friction factor increases monotonously due to the creation of vortices.

4.9. Effect of Arc-shaped ribs

The angle of attack for the arc-shape geometry becomes towards transverse direction for small value of arc angle ($\alpha/90 = 0.3333$) which results in maximum heat transfer coefficient. However, the trend in friction factor has been found reversed. The friction factor has been observed maximum for maximum value of relative arc angle ($\alpha/90$). This could be the advantage of such geometry of artificial roughness with solar air heaters.[40]

4.10. Effect of rib cross section

Rib cross-section affects the size of separated region and level of disturbance in the flow. The friction factor is less for circular cross-section ribs in comparison to that of rectangular or square cross-section ribs on account of reduction in the size of separated region. This results in decrease in inertial losses and increase in skin friction, thereby, decreasing the friction factor. As the size of separated region diminishes, level of disturbance in flow also decreases which affects the heat transfer adversely. Another possible factor contributing to the Nusselt number decrease is the reduction in heat transfer surface area associated with circular cross-section ribs [13]. it is also reported that by changing the rib cross-section from rectangular to trapezoidal the friction factor is reduced; while there is minor effect on reduction of Nusselt number and this effect disappears at higher values of Reynolds number[68].

4.11. Combined turbulence promoter

The groove in inter rib space and nearer the reattachment point of heat transfer surface induces vortices in and around the groove. These vortices increase the intensity of turbulence. The optimum relative roughness pitch is less in comparison to simple ribbed surface; the reported optimum relative groove position g/p is about 0.4.

4.12. Effect of Aspect Ratio

The aspect ratio has effect on the performance of solar air heaters. In large aspect ratio ducts friction is increased with increase in turbulence. The lower aspect ratio duct provides a better heat transfer performance [14]. For equal pumping power, the heat transfer performance of square channel is better than that of rectangular duct with aspect ratio 2 & 3 [15]. The collector efficiency increases with the increase in collector aspect ratio. As the aspect ratio increases, the cross sectional area of the air duct decreases and the velocity of flow increases so the convective heat transfer from the surface of the absorber plate to flowing air increases. In addition to enhancement in heat transfer it also increases the pumping

power of the blower of pump leading to the increase in the operating cost of the equipment [16].

4.13. Effect of Duct height (H)

Solar air heaters with lower duct height have higher efficiency. Lowering of duct height increases the air velocity. The effective efficiency decreases rapidly as the mass flow increases owing to the pumping power requirement which is proportional to ($1/H^3$) [17]. Solar air heater efficiency can be maximized by decreasing the depth of solar air heater along the length but in long channel along the length of the solar air heater causes substantial pressure drop causing high pumping losses[18]. At the optimum channel depth to length ratio the outlet temperature becomes equal to the absorber plate mean temperature [19].

4.14. Effect of Reynolds number

The researchers reported that in case of ribs at low Reynolds number (less than 5000), the value of Nusselt number for the smooth duct is nearly equal to that of rough duct. It is also concluded that smooth duct gives better heat transfer than the artificially roughened duct with ribs at low Reynolds number [24]. It is also reported that for low Reynolds number flow, change in heat transfer coefficient is negligible with respect to roughness pitch, because when Re is low the thermal boundary layer remains unbreakable, which offers resistance to heat flow and hence it may result low heat transfer coefficient [48]. With the increases of Reynolds number, friction factor decreases due to the suppression of viscous sub layer, whereas the Nusselt number increases with increases In Reynolds numbers because it is nothing but the ratio of conductive resistance to convective resistance of heat flow and as Reynolds member increases thickness of boundary layer decreases & hence convective resistance decreases which in turn increases the Nusselt number

4.15. Effect of perforated ribs

In the case of solid ribs, generally a large hot spot is created just behind the downstream of the ribs resulting in heat transfer deteriorate around that position. To overcome this situation perforated ribs were used instead of solid ribs, which enhanced the heat transfer rate. Modified ribs in the form of perforated ribs also decreased the resistance to flow resulting in lower frictional factor.

5. Performance Analysis of solar air heater

5.1 Thermal performance of solar air heater

Thermal performance concerns with heat transfer process within the collector . In order to evaluate thermal performance of a solar air heater, following Hottel–Whillier–Bliss equation reported by Duffie and Beckman [56] is commonly used.

$$q_u = Q_u/A_s = F_R [I (\tau\alpha)_e - U_L (T_i - T_a)] \text{----------1}$$

The rate of useful energy gain by the flowing air through duct of a solar air heater may also be calculated by :

$$Q_u = mC_p(T_o - T_i) = hA_s(T_{pm} - T_{fm}) \text{----------2}$$

As discussed , heat transfer coefficient (h) is represented in non-dimensional form by Duffie & Beckman [56].

$$Nu = hL/k \text{----------3}$$

Furthermore thermal efficiency of a solar air heater can be expressed by the following equation:

$$\eta_{th} = q_u/I = F_R[(\tau\alpha)_e - U_L\{(T_i - T_a)/I\}] \text{----------4}$$

The above equation shows that the plot between η_{th} and parameter $\{(T_i - T_a)/I\}$ can be approximated by a straight line, of which intercept and slope are given by the values of $F_R(\tau\alpha)_e$ and $F_R U_L$ respectively.

5.2 Hydraulic Performance

Hydraulic performance of a solar air heater concerns with pressure drop (ΔP) in the duct. Pressure drop accounts for energy consumption by fan to propel air through the duct. Pressure drop can be represented in non-dimensional form by using the following relationship of friction factor (f), reported by Frank and Mark [57].

$$f = \Delta P D_h / 2\rho L V^2 \text{----------5}$$

5.3 Thermo Hydraulic Performance

It is desirable that design of collector should be made in such a way that it should transfer maximum heat energy to the flowing fluid with minimum consumption of fan energy. Therefore in order to analyze overall performance or to measure the relevance of use of artificial roughness on absorber plate , thermo hydraulic performance should be evaluated by considering thermal & hydraulic characteristics of the collector simultaneously. The parameter that facilitates simultaneous consideration of thermal and hydraulic performance is given by various researchers as Webb and Eckert [58] and Lewis [59] as

$$\eta = (Nu_r/Nu_s)/(f_r/f_s)^{1/3} \text{----------6}$$

This parameter is in fact is the ratio of Nusselt number ratio of roughened surface to smooth surface and friction factor ratio of roughened surface to smooth surface. The higher value, greater than one i.e.(>1) of this parameter is always

desirable for justifying the use of artificial roughness in the solar air heaters or duct. The higher the value the better is the performance. It shows the comparative increase in the Nusselt number to the friction factor of roughened surface in comparison with the smooth surface. This parameter is also used to compare the performance of various roughness elements arrangement combinations to obtain the best one.

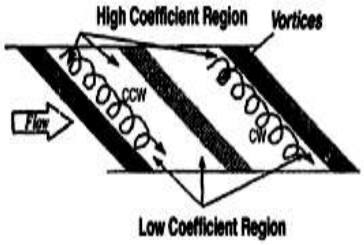

Fig.8. Effect of angled ribs

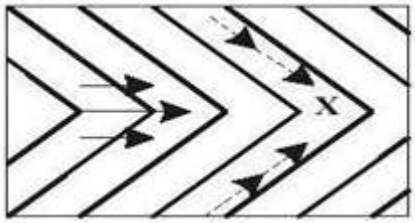

Fig.9. Generation of secondary flow along different ribs

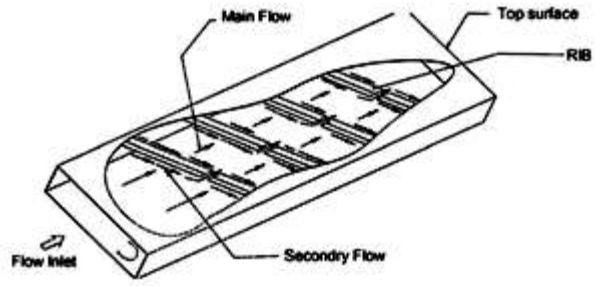

Fig.10. Effect of position of gap in inclined rib

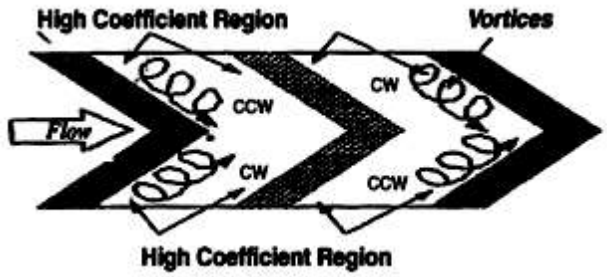

Fig.11. Effect of V-shaping ribs

6. Different types of roughness geometries used in solar air heater

There were so many types of roughness geometry that have been explored and examined by various investigators in order to enhance the heat transfer. Roughness in the form of ribs, wire matrix and dimples were mainly suggested by different investigators to achieve better thermal performance. Among all, rib roughness was found the best performer as far as thermal performance is concerned. Various types of artificial roughness geometry are discussed below.

6.1. Transverse continuous ribs

Kays [20] proposed fixing small diameter protrusion wires perpendicular to flow direction on surface of absorber plate break laminar sub-layer. It was suggested that protrusion wire diameter of y^+=50, spaced 10–20 times diameter and placed within the laminar sub-layer are better than turbulence promoters.

Prasad and Mullick [21] investigated on solar air heater with protruding wires in underside of the absorber plate. They found improvement of 9% (from 63% to 72%) in plate efficiency (FP) for Reynolds number of 40000. The plate efficiency is 44.5% higher in cross corrugated sheet with protruding wire than plane galvanized iron sheet.

Prasad and Saini [7,8] develop empirical correlations for heat transfer coefficient and friction factor for fully developed turbulent flow in a solar air heater duct having absorber plate roughened artificially by small diameter wires as shown in Fig.12 of various relative roughness heights ranging from 0.020 to 0.033 and relative roughness pitch varying from 10 to 20 for Reynolds numbers range between 5000 and 50,000. It was found that the average friction factor & Nusselt number increased with increase in relative roughness height. The average Nusselt number of the roughened duct was about 2.10, 2.24 and 2.34 times than that of the smooth duct for relative roughness height of 0.020, 0.027 and 0.033 respectively. The average friction factor of the roughened duct was about 3.08, 3.67, and 4.26 times than that of the smooth duct. The increase in the average Nusselt number & friction factor for relative roughness pitch of 10, 15 & 20 in the roughened duct was about 2.38, 2.14, 2.01 & 4.25, 3.39, 2.93 times than that of the smooth duct respectively.

Gupta et al. [22] studied effect of transverse wire roughness on heat and fluid flow characteristics for solar air heater ducts with an absorber plate having transverse wires fixed on the underside of it as shown in Fig.12 for Reynolds number range of 3000–18,000, duct aspect ratio of 6.8–11.5, relative roughness height of 0.018–0.052 at a relative roughness pitch of 10 with a range of roughness Reynolds number between 5 and 70. It is found that Stanton number increased initially with an increase in Reynolds number up to 12000 and registered a slight fall thereafter.

Verma and Prasad [23] carried out an outdoor experimental investigation for thermo hydraulic optimization of the roughness and flow parameters for Reynolds number (Re) range of 5000–20,000, relative roughness pitch (p/e) range of 10–40 and relative roughness height (e/D_h) range of 0.01–0.03. The optimal value of roughness Reynolds number (e+) was found to be 24 and corresponding to this value, optimal thermo hydraulic performance was reported to be 71%. Heat transfer enhancement factor was found to vary between 1.25 and 2.08 for the range of parameters investigated as in Fig 12.

6.2. Transverse broken ribs

Sahu and Bhagoria [24] investigated the effect of 90^0 broken ribs on thermal performance of a solar air heater for fixed roughness height (e) value of 1.5 mm, duct aspect ratio (W/H) value of 8, pitch (p) in the range of 10–30 mm and Reynolds number (Re) range of 3000–12,000. Roughened absorber plate increased the heat transfer coefficient by 1.25 to 1.4 times as compared to smooth one under similar operating conditions. Corresponding to roughness pitch (p) value of 20 mm, maximum value of Nusselt number was obtained that decreased on the either side of this roughness pitch (p) value. Based on the experimental investigation, the thermal efficiency of roughened solar air heater was found to be in the range of 51–83.5% depending upon the flow conditions. The geometry investigated has been shown in Fig.13.

6.3. Inclined continuous ribs

Han and Park [25] investigated the effect of angled or inclined ribs on heat transfer and friction factor in narrow aspect ratio ducts & found that the angled ribs result in higher heat transfer compared to the transverse ribs, because of the secondary flow induced by the rib angle in addition to breaking of the laminar sub-layer & producing local wall turbulence.

Gupta et al. [26] experimentally investigated the effect of relative roughness height (e/D_h), inclination of rib with respect to flow direction & Reynolds number on the thermo hydraulic performance of a roughened solar air heater for transitionally rough flow region ($5< e+ <70$) as shown in Fig. 14. It was reported that with increase in relative roughness height (e/D_h), the value of Reynolds number decreased for which effective efficiency was maximum. The effective efficiency also increased with increase in insolation. For a roughened solar air heater, maximum enhancement in heat transfer and friction factor was reported to be of the order 1.8 and 2.7 times respectively corresponding to angle of inclination values of 60^0 and 70^0, respectively. Best thermo hydraulic performance was reported for (e/D_h) value of 0.023 & (Re) value of 14,000.

Lu and Jiang [27] investigated experimentally heat transfer of air in a rectangular channel with 45^0 angled ribs on one wall. They also investigated numerically heat transfer and friction factor of inclined ribs with 0^0, 10^0, 20^0, 30^0, 45^0, 60^0& 90^0. The numerical results showed that the heat transfer coefficients were highest with the 60^0 angled ribs, but the channel with the 20^0 angled ribs had the best overall thermo-hydraulic performance when the spacing between ribs was 4 mm.

6.4. Inclined broken ribs

Aharwal et al. [28] experimentally studied the effect of width and position of gap in inclined split-ribs having square cross-section on heat transfer & friction factor of a rectangular duct as in Fig.15. The duct had an aspect ratio (W/H) of 5.84, (p/e) of 10, (e/D_h) of 0.0377, angle of attack (α) of 60^0, relative gap width (g/e) range of 0.5–2 and relative gap position (d/W) varied from 0.1667 to 0.667 for (Re) range of 3000–18000. For the split-rib and continuous rib roughened ducts, the enhancement in heat transfer was reported to be in the range of 1.71–2.59 & 1.48–2.26 times respectively over smooth duct under similar conditions. The maximum values of heat transfer, friction factor ratio (f_r/f_s) and thermo hydraulic parameter so obtained were corresponding to (g/e) value of 1.0 and relative gap position (d/W) value of 0.25 for the range of parameters investigated. Particle Image

Kumar et al. [29] experimental study has been carried out for enhancement of heat transfer coefficient of a solar air heater having roughened air duct provided with artificial roughness in the form 60^0 inclined discrete rib as in Fig.16. Reynolds number ranges from 4105.2 - 20526.2, (e/D_h) ranges from 0.0249 - 0.0498, (p/e) ranges from 8-16, Relative gap position (d/W) ranges from 0.15-0.35, Relative gap width (g/e) of 1, Considerably enhancement in heat transfer coefficient has been achieved with such roughness element. The enhancement in Nusselt number & Friction factor is 2.57 and 3.72 times the smooth surface. The maximum heat transfer enhancement occurs for the relative roughness pitch of 12, relative gap position of 0.35 & relative roughness height of 0.0498.

6.5. Combination of inclined and transverse ribs

Varun et al. [30] carried out an experimental study on heat transfer and friction characteristics by using a combination of inclined and transverse ribs on the absorber plate of a solar air heater as shown in Fig 17, with (Re) ranging from 2000 to 14,000, (p/e) range of 3–8, (e/D_h) value of 0.030, duct aspect ratio (W/H) value of 10 & roughness height (e) value of 1.6 mm. For (p/e) value of 8, the best thermal performance was reported..

6.6. V-shaped continuous ribs

Momin et al. [31] experimentally investigated the effect of geometrical parameters of V-shaped ribs, shown in Fig. 18, on heat transfer and fluid flow characteristics of rectangular duct of a solar air heater. The investigation covered a (Re) range of 2500–18000, (e/D_h) range of 0.02–0.034 and angle of attack of flow (α) range of $30–90^0$ for a fixed (p/e) value of 10. Rate of increase of Nusselt number was observed to be lower than the rate of increase of friction factor with an increase in Reynolds number. The maximum enhancement of Nusselt number and friction factor as result of providing

artificial roughness had been found to be 2.30 and 2.83 times respectively over the smooth duct for an angle of attack (α) of 60^0. It was reported that for (e/D_h) value of 0.034 and angle of attack (α) of 60^0, v-shaped ribs enhanced the value of Nusselt number by 1.14 and 2.30 times over inclined ribs and smooth absorber plate respectively.

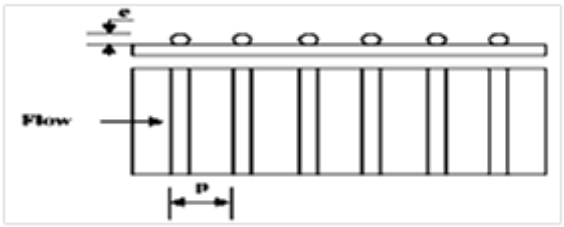

Fig.12. Transverse ribs by Prasad & Saini

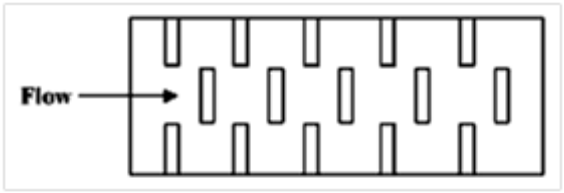

Fig.13. Transverse Broken ribs

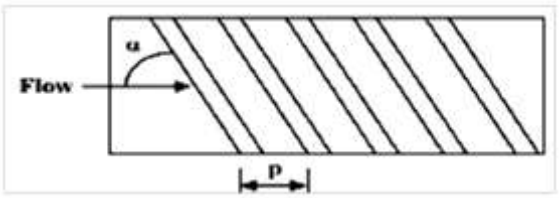

Fig. 14. Inclined continuous ribs

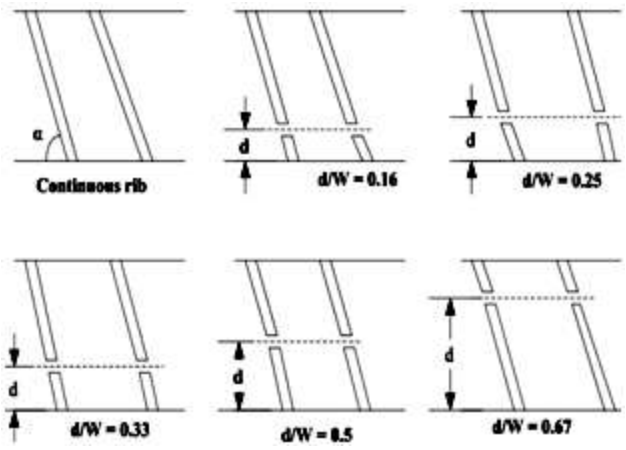

Fig. 15. Various types of Inclined Broken ribs

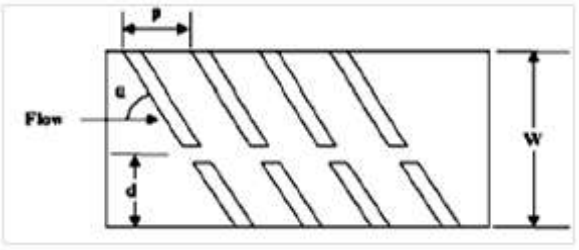

Fig. 16. Inclined broken ribs by kumar et al

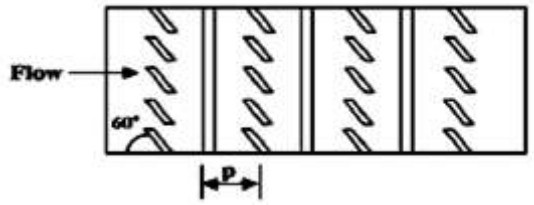

Fig. 17 Combined inclined & transverse ribs

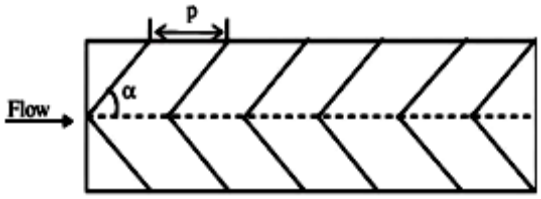

Fig.18. V-shaped ribs

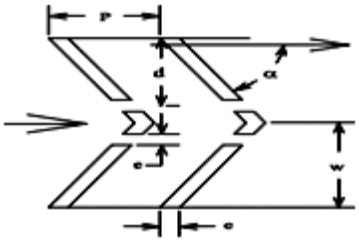

Fig.19. Discrete V-down rib

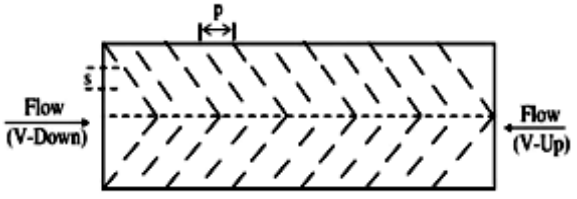

Fig. 20 V-shaped staggered discrete ribs

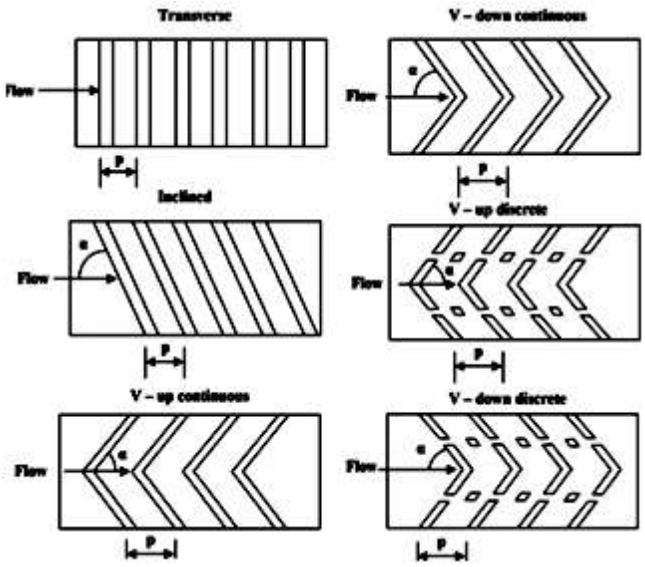

Fig.21. Different types of ribs by Karwa

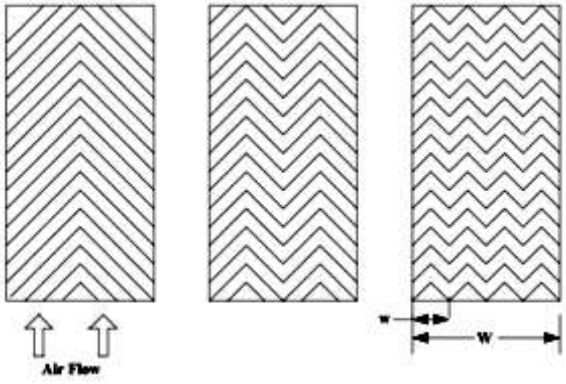

Fig. 22 Multiple V-ribs by Hans

6.7. V-shaped discrete ribs

Singh et al. [32,33] experimentally investigated the heat & fluid flow characteristics of rectangular duct having its one broad wall heated & roughened with periodic 'discrete V-down rib' as in Fig 19. As Reynolds number is increased, the Nusselt number increase is more for discrete V-down rib as compared to continuous V-down rib. This is probably due to increase in local Nusselt number downstream of gap caused by increased flow velocity through the gap. It is observed that at all Reynolds number, the Nusselt number increases with increase in relative roughness pitch (p/e) up to the value of 8.0 and then reduces as (p/e) is increased further. It is observed that at all Reynolds number, the Nusselt number increases as relative gap width (g/e) is increased from 0.5 to 1.0 and thereafter it decreases as (g/e) is increased further. The value of Nusselt number is found to be highest at angle of attack (α)=60^0. Also maximum value of Nusselt number is recorded at relative gap position(d/w) of 0.65.

6.8. V-shaped staggered discrete ribs

Muluwork et al. [12] compared the thermal performance of staggered discrete V-apex up and down ribs with corresponding transverse staggered discrete ribs shown in Fig. 20. They studied the effect of relative roughness length ratio (B/S), relative roughness segment ratio (S'/S), relative roughness staggering ratio (p'/p) and angle of attack (α) on the heat transfer and friction factor. It was observed that the Nusselt number increased with the increase in relative roughness length ratio (B/S). Nusselt number for V-down discrete ribs was found to be higher than the corresponding V-up and transverse discrete roughened surfaces. Nusselt number increased with increase in relative roughness staggering ratio (p'/p) and attained a maximum value for relative roughness staggering ratio (p'/p) value of 0.6. Heat transfer and friction factor attained maximum values for angle of attack (α) 60^0 and 70^0, respectively.

6.9. Transverse, Inclined, V-cont. & discrete rib roughness

Karwa [34] carried out a comparative experimental study of augmented heat transfer and friction in a rectangular duct with rectangular cross-section ribs arranged in V-continuous & V discrete pattern for duct aspect ratio (W/H) range of 7.19–7.75, relative roughness pitch (p/e) value 10, relative roughness height (e/D_h) range of 0.0467–0.050 and Reynolds number range of 2800–15000. as in Fig 21. The enhancement in the Stanton number over the smooth duct was reported to be in range of 102–137%, 110–147%, 93–134% and 102–142% for transverse, inclined, V-up continuous, V-down continuous, V-up discrete and V-down discrete rib respectively. The friction factor ratios corresponding to these arrangements were found as 3.02–3.42, 3.40–3.92, 3.32–3.65, 2.35–2.47 and 2.46–2.58, respectively. The performance of V-down ribs was observed to be better than that of V-up ribs, which was in confirmation with the findings of Muluwork et al. [44].

6.10. Multiple V ribs

Hans et al. [35] carried out an experimental investigation to study the effect of multiple v-rib roughness as shown in Fig. 22 on heat transfer coefficient & friction factor in an artificially roughened solar air heater duct. A maximum enhancement of Nusselt number & friction factor due to presence of such an artificial roughness has been found to be 6 and 5 times, respectively, in comparison to the smooth duct for the range of parameters considered. The maximum heat transfer enhancement has been found to occur for a relative roughness width (W/w) value of 6,while friction factor attains maximum value for relative roughness width (W/w) value of 10.It has also been found that Nusselt number and friction factor attain maxima corresponding to angle of attack(α) of 60^0& a (p/e) of value of 8.

6.11. Multi V shape ribs with gap

Kumar et al. [11,55] further extended the previous authors work with V-shaped rib and investigated with multiple V shape rib with a gap as shown in Fig.23 and concluded that

the maximum enhancement in Nusselt number and Nusselt number ratio (Nu_r/Nu_s) as well as friction and friction factor ratio (f_r/f_s) occurs at relative gap width (g/e) of 1 and relative gap distance (G_d/L_v) of 0.69. Relative gap distance has more effect on increasing the heat transfer as it increases the strength of the secondary flow simultaneously the secondary flow influences the axial flow profile thus increasing the frictional effects.

6.12. W-shaped rib

Lanjewar et al. [36,37] investigated the thermo-physical behaviour of the W-shaped ribs of different orientation on the absorber plate as shown in Fig.24. The duct had a aspect ratio (W/H) of 8, (p/e) of 10, (e/Dh) of 0.03375 and angle of attack of flow (α) of 300–750. They concluded that W down ribs give the higher thermo-hydraulic performance (Nur/Nus)/(fr/fs) at (e/Dh) of 0.03375, P/e of 10 and α of 600. They further concluded that the W down ribs were better than W up ribs. They also made the study on W-shaped ribs with increment in Nu & friction factor of 2.36 & 2.01.

6.13. Discrete W-shaped ribs

Kumar et al. [38,39] carried out an experimental investigation to determine the heat transfer distributions in solar air heater having its absorber plate roughened with discrete w-shaped ribs a shown in Fig 25. The experiment encompassed (Re) ranges from 3000 to 15000, rib height (e) values of 0.75- 1 mm, (e/Dh) 0.0168 & 0.0225 & (p/e) of 10 and angle of attack (α) 450. Thermal performance of roughened solar air collector was compared with that of smooth one under similar flow conditions and it was reported that thermal performance of the roughened channel was 1.2–1.8 times the smooth channel for range of parameters investigated. Discretization was found to have significant effect on heat transfer enhancement. Nu & friction factor was reported as 2.16 & 2.75 times that of smooth duct, at angle of attack of 600 & (e/Dh) of 0.0338.

6.14. Arc shaped ribs

Saini and Saini [40] studied the effect of arc shaped ribs on the heat transfer coefficient & friction factor of rectangular ducts with (Re), (e/Dh) & relative arc angle (α) varying from 2000 to 17000, 0.0213 to 0.0422 & 0.3333 to 0.6666, respectively as shown in Fig 26. It was reported that relative arc angle (α) had an opposite effect on heat transfer enhancement and friction factor. With decrease in relative arc angle (α) value, Nusselt number value increased while friction factor value decreased. Enhancement of Nusselt number and friction factor was reported to be of order 3.6 and 1.75 times respectively over smooth duct for relative arc angle (α) value of 0.3333 & (e/Dh) of 0.0422.

6.15. Broken arc ribs

V.S. Hans et al.[41] investigated Heat transfer & friction factor correlations for a solar air heater duct roughened artificially with broken arc ribs as shown in Fig.27. The experiments encompasses Re in the range of 2000–16000, Relative gap position (d/w) 0.20–0.80, Arc-angle (α) 15–75^0, Relative gap width (g/e) 0.5–2.5, (p/e) 4–12, (e/D_h) 0.022–0.043 & aspect ratio of 12. The maximum increase in Nusselt number & friction factor over that of continuous arc rib roughened duct was 1.19 & 1.14 times respectively. The corresponding values over that of smooth duct were 2.63 & 2.44 times respectively. The maximum enhancement occurs at relative roughness pitch of 10, relative gap width of 1.0, arc angle of 30^0, relative gap position of 0.65 and relative roughness height of 0.043.

6.16. Broken Arc Shape with Staggered Rib Pieces

R S Gill et al.[42] investigated heat transfer & Friction Factor of Solar Air Heater duct Roughened by Broken Arc Shaped Ribs Combined with Staggered Rib Piece as shown in Fig.28. The experiments carried out encompasses Reynolds number in the range of 2000–16000, relative roughness height (e/D_h) 0.043, arc angle (α) 30^0 and Relative gap width, (g/e) in the range of 0.5-2.5, Relative gap position, (w'/w) 0.65, Relative staggered rib position, p'/p 0.6, Relative staggered rib size, r/g 2.0, Relative roughness pitch, p/e 10. The highest enhancement in Nusselt number is 177% at Reynolds number of 12000 with corresponding enhancement in friction factor of 137%. The highest thermo-hydraulic parameter obtained is 2.08 corresponding to relative gap width of 1.0 at (Re) of 12000.

6.17. Multiple Arc shaped ribs

A.P. Singh et al.[43] investigated Heat transfer and friction factor correlations for multiple arc shape roughness elements on the absorber plate used in solar air heaters as shown in Fig.29. The experiments carried out encompasses Reynolds number in the range of 2200–22,000, relative roughness height (e/D_h) values of 0.018–0.045, arc angle (α) range of 30–75^0 and relative roughness width (W/w) ranges from 1 to 7 and relative roughness pitch (p/e) range of 4-16. A maximum enhancement obtained in Nusselt number and friction factor is 5.07 and 3.71 respectively for multiple arc-shaped roughness geometry as compared to smooth one. The maximum enhancement for Nu takes place at Re of 22,300, relative roughness width (W/w) value of 5, (e/D_h) value of 0.045, (p/e) value of 8 and relative arc angle (α/90) value of 0.667 while maximum friction factor takes place at Re of 22300, relative roughness width (W/w) value of 7, (e/D_h) of 0.045, (p/e) value of 8 and relative arc angle (α /90) value of 0.667.

6.18. Multiple Arc shaped ribs with gap

N.K. Pandey et al. [44] investigated heat transfer augmentation using multiple arcs with gap on absorber plate of solar air heater as shown in Fig.30. The investigation encompassed Reynolds number ranges from 2100 to 21000, relative roughness height (e/D_h) ranges from 0.016 to 0.044 , relative roughness pitch (p/e) ranges from 4 to 16 , arc angle (α) values are 30–75^0 , relative roughness width (W/w) ranges from 1 to 7, relative gap distance (d/x) values are 0.25–0.85 and relative gap width (g/e) ranges from 0.5 to 2.0. The

maximum increment in Nusselt number & friction factor (f) is 5.85 and 4.96 times in comparison to the smooth duct. The maximum enhancement for Nu takes place at (Re) value of 21000, g/e value of 1, d/x value of 0.65, W/w value of 5, e/D_h value of 0.044, p/e value of 8 and α /60 value of 1.

6.19. Rib grooved roughness

Jaurker et al. [45] experimentally investigated heat transfer & friction factor of rib-groove roughened rectangular duct as shown in Fig. 31. The effect of (p/e), (e/D_h) & relative groove position (g/p) on the heat transfer coefficient & friction factor had been studied. The presence of rib-grooved artificial roughness yielded Nusselt number & friction factor up to 2.7 and 3.6 times respectively in comparison to smooth plate. The maximum heat transfer occurred for a (p/e) of 6 & (g/p) value of 0.4.

6.20. Chamfered rib grooved roughness

Layek et al. [46] carried out an experimental investigation to study heat transfer and friction for repeated transverse compound rib-groove arrangement on absorber plate of a solar air heater as in Fig 32. Four relative rib-groove positions (g/p) values of 0.3, 0.4, 0.5 and 0.6 were investigated for fixed relative roughness height (e/D_h) and relative roughness pitch (p/e) values of 0.03 and 10 respectively. It was found that corresponding to relative roughness pitch (p/e) value of 10, relative groove position (g/p) value of 0.4 provided about 2.42 and 2.6 times increase in the Nusselt number and friction factor respectively for entire range of Reynolds number studied.

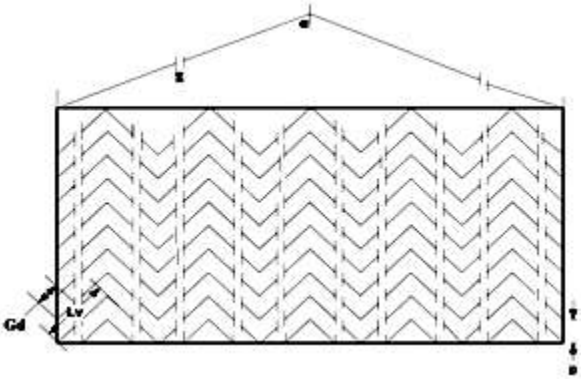

Fig.23 Multi V-rib with gaps

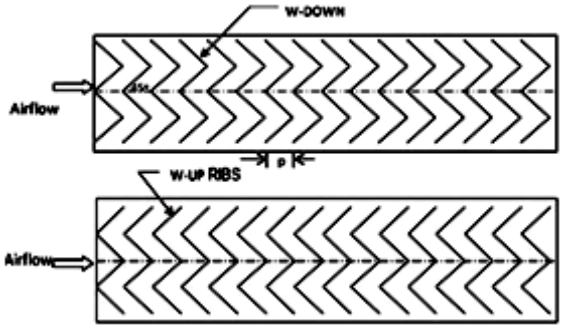

Fig. 24. W-shaped ribs .

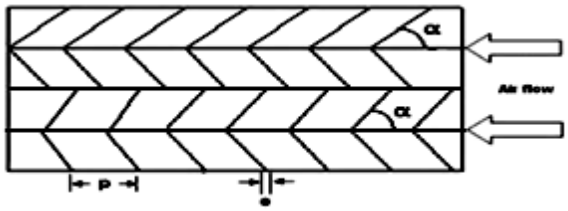

Fig. 25. Discrete W-shaped ribs

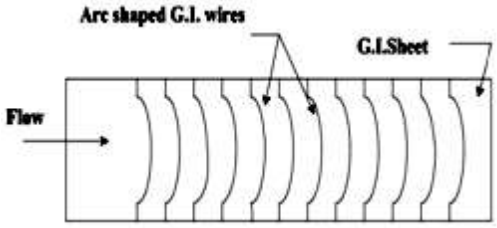

Fig. 26 Arc shaped ribs

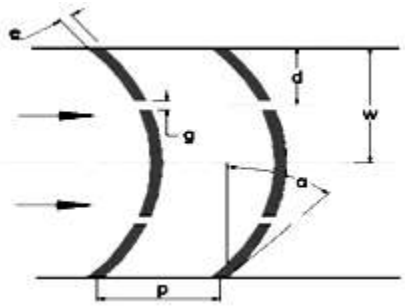

Fig. 27. Broken arc ribs

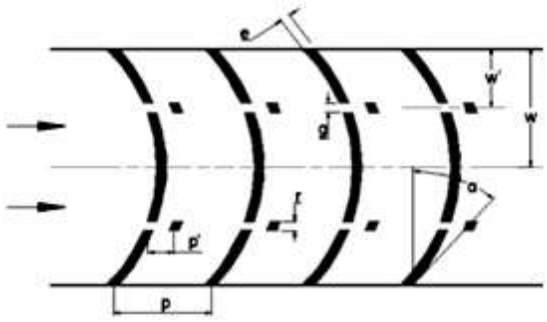

Fig.28 Broken Arc Shape with Staggered

 ISSN: 2321-8169
186 - 206

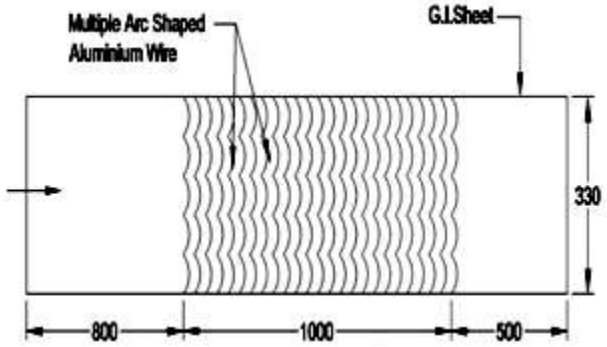

Fig. 29 Multiple Arc shaped ribs

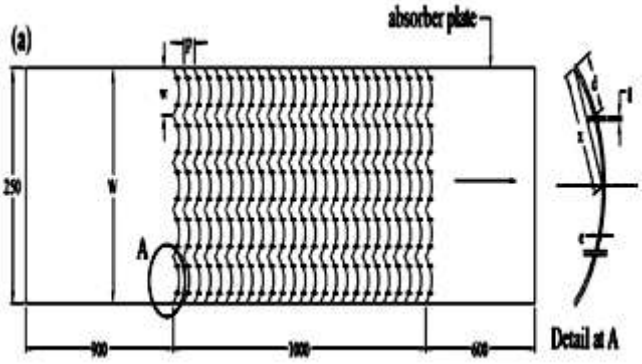

Fig.30. Multiple Arc shaped ribs with gap

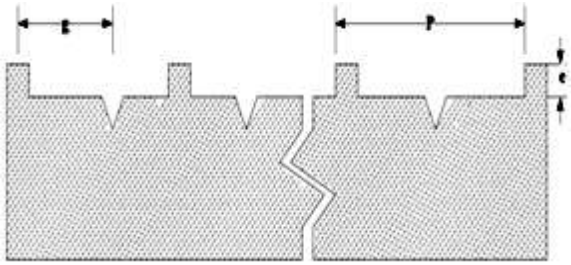

Fig.31 Rib grooved roughness

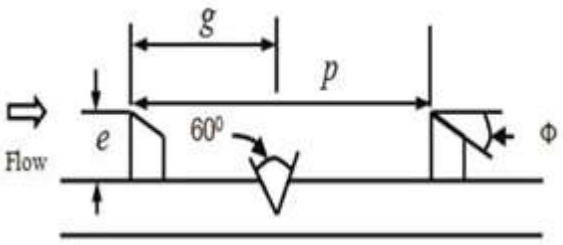

Fig.32 Chamfered rib grooved roughness

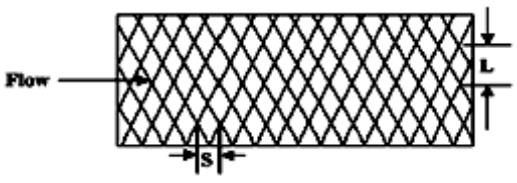

Fig. 33 Expanded mesh metal

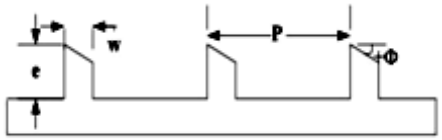

Fig.34 Chamfered ribs

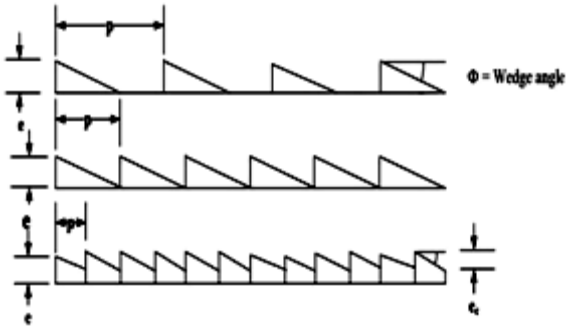

Fig.35 Wedge shaped ribs

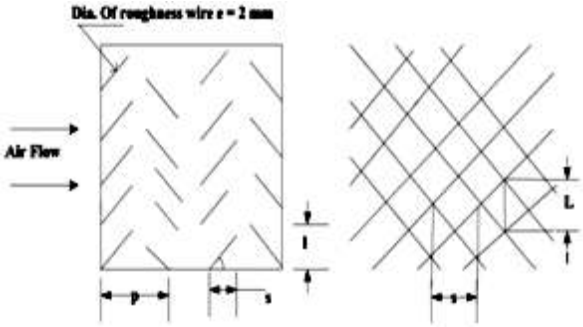

Fig 36. Metal grit ribs

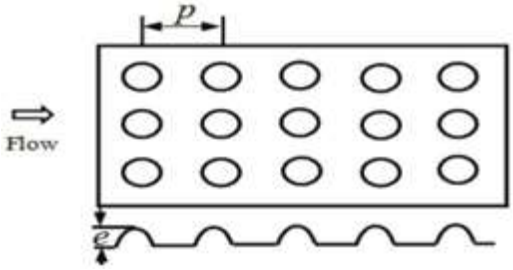

Fig.37 Dimple shape roughness by Protrusions

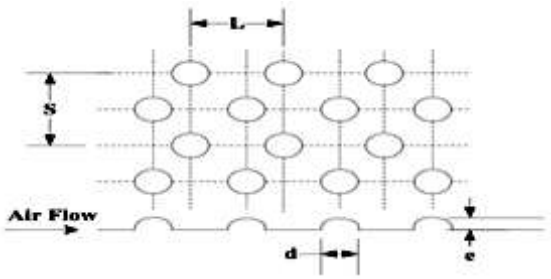

Fig.38 Roughness by Bhusan & Singh

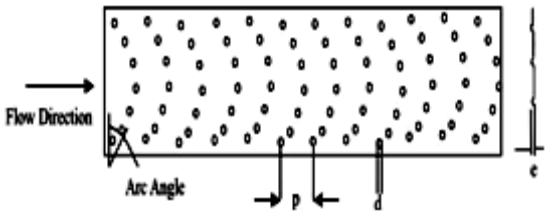

Fig.39 Dimple surface in arc manner

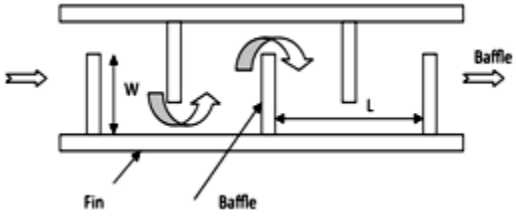

Fig. 40 Baffles attached to absorber plate

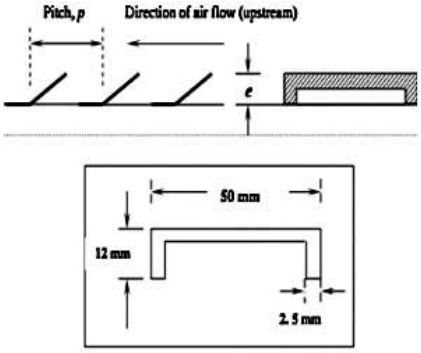

Fig. 41 U shaped turbulators

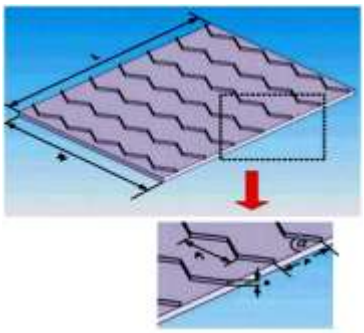

Fig.42 Multiple v shaped baffles

6.21. Expanded mesh metal

Saini and Saini [47] carried out an experimental investigation to study the effect of wire mesh roughened absorber plate on heat transfer augmentation and friction characteristics of solar air heater as shown in Fig.33. The investigation considered relative longway length of mesh (L/e) in range of 25–71.87, relative shortway length of mesh (S/e) in range of 15.62–46.87, relative roughness height (e/D_h) in range of 0.12–0.039 & (Re) in range of 1900–13,000. It was reported that the maximum heat transfer of order 4 times over the smooth duct was obtained corresponding to angle of attack of 61.9^0, relative longway length of mesh (L/e) value of 46.87 and relative shortway length of mesh (S/e) value of 25. Maximum value of friction factor was reported for angle of attack of 72^0, relative longway length of mesh (L/e) value of 71.87 and relative shortway length of mesh (S/e) value of 15.

6.22. Chamfered ribs

Karwa et al. [14] performed an experimental investigation of heat transfer and fiction for rectangular ducts, having aspect ratio (W/H) in the range of 4.8–12, and roughened with repeated integral chamfered ribs, as shown in Fig. 34. The roughness parameters considered for the investigation were (Re) range of 3000–20,000, relative roughness height (e/D_h) range of 0.014–0.0328, relative roughness pitch (p/e) range of 4.5–8.5 and chamfer angle (ϕ) varying from 15^0 to 18^0. Stanton number and friction factor increased with increase in chamfer angle and attained maximum value corresponding to chamfer angle (ϕ) value of 15^0. It was reported that Stanton number decreased while friction factor increased with increase in aspect ratio (W/H). As compared to smooth duct, the presence of chamfered ribs on the wall of duct yielded up to about two-fold and three-fold increase in the Stanton number and the friction factor respectively in the range of parameters investigated. Heat transfer and friction factor correlations were developed.

6.23. Wedge shaped ribs

Bhagoria et al. [48] experimentally studied heat transfer & flow characteristics in a solar air heater having absorber plate roughened with wedge shaped transverse integral ribs as shown in Fig. 35. The investigation encompassed the Reynolds number range of 3000–18,000, relative roughness height (e/D_h) range of 0.015–0.033 and rib wedge angle (ø) range of 8–128. It was reported that Nusselt number and friction factor increased by 2.4 and 5.3 times over smooth duct in the range of parameters investigated.

6.24. Metal grit ribs

Karmare and Tikekar [49] experimentally investigated heat transfer & friction characteristics of a rectangular duct having absorber plate roughened with a defined grid of metal ribs of circular cross-section and the roughness geometry investigated has been shown in Fig. 36. The investigation considered relative roughness height (e/D_h) range of 0.035–0.044, relative roughness pitch (p/e) range of 12.5–36, relative grit length (l/s) range of 1–1.72 & (Re) range of 4000–17000. Enhancement in Nusselt number was found to be 187% & the friction factor increased by 213% & optimum performance was observed for relative grit length (l/s) value of 1.72, (e/D_h) value of 0.044 & (p/e) value of 17.5 for the range of parameters studied.

6.25. Dimpled surfaces

Saini and Verma [50] studied the effect of roughness and operating parameters on heat transfer and friction factor in a

roughened duct provided with dimple-shape roughness geometry as shown in Fig. 37, for the range of (Re) from 2000 to 12,000, (e/D_h) from 0.018 to 0.037 and (p/e) from 8 to 12. For the range of parameters investigated, Nusselt number was found to be maximum corresponding to (e/D_h) value of 0.0379 and (p/e) value of 10. For fixed value of (p/e) of 10, friction factor attained the maximum and minimum values corresponding to (e/D_h) values of 0.0289 and 0.0189, respectively.

Bhusan and Singh [51] investigated the solar air heater with protrusion on the absorber plate as shown in Fig. 38. They concluded that the heat transfer coefficient increases as compared to smooth surface, which may be due to main flow impingement, vortex generation on both sides of the protrusion and flow separation. The performance is highest at relative shortway length (S/e) of 31.25 & relative longway length (L/e) of 31.25.

Yadav et al. [52] employed Dimple shaped roughness in arc shaped manner roughness geometry as shown in Fig. 39. Experiment encompassed Reynolds number range from 600to 18100, p/e as 12 to 24, e/D_h as 0.015 to 0.03 and arc angle of protrusion arrangement as $45–75^0$. Maximum enhancement of Nusselt number and friction factor was found to be 2.89 and 2.93 times smooth duct for range of parameters investigated. Maximum heat transfer enhancement & friction factor occurred for relative roughness height of 0.03, relative roughness pitch of 12 and for arc angle of 60^0.

Sethi et al. [53] investigated Dimple shaped roughness but with different set of parameters roughness geometry is same as shown in Fig. 39. Investigation covered duct aspect ratio 11, (p/e) of 10–20, relative roughness height 0.021–0.036, arc angle $45–75^0$& (Re) from 3600–18,000. They reported maximum value of Nusselt number corresponded to relative roughness height of 0.036,relative roughness pitch (p/e) value of 10 and arc angle (α) value of 60^0.

7. Baffles

7.1. Solid baffles

The uses of turbulators in the cooling channel or channel heat exchanger such as ribs, grooves or baffles are introduced in order to increase the convective heat transfer rate leading to the compact heat exchanger and increasing the efficiency. Periodic flow interruption by baffle arrays mounted periodically on the walls is an extensively used means for augmentation of heat transfer in many industrial applications. The baffles completely make the change of flow field and thus the distribution of local heat transfer coefficient. The baffle increases the degree of heat transfer coefficient and restarts the boundary layer after flow reattachment between baffles. The heat transfer increase is associated with increase in pressure drop due to increase in flow area effects. Thus the geometry parameters are the most important concern of design and the designers are looking towards the optimum parameters and geometry of baffles and their arrangements.[60]

Yeh and Chou [61] experimentally investigate the efficiency of solar air heaters with baffles as shown in Fig. 40 and found considerable improvement in the collector efficiency of solar air heaters with fins in the collector are provided with attached baffles to create air turbulence and an extended heat transfer area and on increasing the density of baffles i.e. either increasing W/De or decreasing l/L also increases the collector efficiency but this will increase power consumption.

Bopche and Tandale [62] carried out experimental investigation to study heat transfer & friction factor by using artificial roughness by using U shaped turbulators on the absorber surface as in Fig. 41 of an air heater duct over the range of parameters Re: 3800–18000, e/Dh = 0.0186–0.03986, p/e = 6.67–57.14,α = 90◦. It was observed that roughness pitch strongly affects the flow pattern and hence the performance of the duct. The turbulators geometry shows appreciable heat transfer enhancement even at low Reynolds number i.e. Re < 5000 where ribs are inefficient. At Reynolds number Re = 3800, the maximum enhancement in Nusselt number and friction factor are of the order of 2.388 and 2.50 respectively and the maximum enhancement in Nusselt number and friction factor values compared to smooth duct are of the order of 2.82 & 3.72 respectively.

Promvonge [63] carried out experimental investigation of heat transfer and friction factor characteristics of a rectangular duct of AR = 10 with multiple 60◦ V baffles as shown in Fig. 42 and the range of parameters investigated are e/H = 0.10, 0.20, 0.30, P/H = 1–3, Re: 5000–25,000. It was found that Nusselt number augmentation tends to increase with the rise of Reynolds number. The use of V baffles with e/H = 0.30 causes a very high heat transfer and pressure drop increase as compared with outer flow blockage ratios. In similar e/H it is clear that V baffles with PR = 1 give much higher heat transfer rate and friction factor than with PR = 2 and 3. For comparison in terms of thermal enhance factor, the use of V baffle with e/H = 0.10. leads to the highest value and is about 1.87 at PR = 1 and the lowest value of Reynolds number.

Sriromreun et al. [64] investigated experimentally and numerically the influence of baffle turbulators on heat transfer augmentation in a rectangular channel of aspect ratio of 10 fitted with the in-phase and out-phase 45^0 Z-baffles in the turbulent regime from Re=4400 to 20,400 as in Fig.43. Effects of the Z-baffle height and pitch spacing length were examined to find the optimum thermal performance for the Reynolds number from 4400 to 20,400.The Z-baffles inclined to 45^0 relative to the main flow direction were characterized at three baffle to channel-height ratios (e/H=0.1,0.2and 0.3) and baffle pitch ratios(P/H=1.5, 2 and 3). For the in-phase baffle array at P/H=1.5,the increases in Nu with the e/H=0.1,0.2 and 0.3 were in the range of 430–440%,530–550% and 640–670% over the smooth channel, respectively. More- over, the use of Z-baffles with e/H=0.3 were reported to give higher heat transfer than that with e/H=0.2 and 0.1 around 10% and 30%,respectively.The friction factor value of

the Z-baffle at P/H=1.5 and e/H=0.3 was found to be around 2 and 5 times higher than that with e/H=0.2 and 0.1,respectively. For the in phase Z-baffle at e/H=0.1, the increases of the Nu for P/H=1.5,2 and 3 were in a range of 430–440%,310–380% and 310–330% over the smooth channel, respectively. Importantly, the Z-baffle with e/H=0.1 at P/H=1.5 shows higher heat transfer rate than the one at P/H=2 and 3 around 15% and 30%,respectively.

7.2. Perforated baffles

Roughness elements of larger height give a high increase in the heat transfer but increase in pressure drop is a serious concern. Hot zones develop in the wake of these elements because of recirculation flow. This leads to lower heat transfer from these zones, thus an attempt has been made by the designers to overcome this effect by putting perforation in the baffles which increase the heat transfer from these zones and help in reducing the pressure drop across the channel. The perforated elements allow a part of the flow to pass through these perforations and thus the hot zones and form drag are reduced[60].

Karwa et al. [65] experimentally investigate the heat transfer and friction in rectangular ducts with transverse baffles solid or perforated as shown in Fig. 44 attached to one broad wall and range of parameters investigated are P/e: 29, e/H: 0.495 and Re: 2850–11,500 and study reveals the enhancement of 73.7–82.7% in 'Nu' over smooth duct for solid baffles & from 60.6–62.9% to 45–49.7% for the perforated baffles and friction factor for the solid baffles is found to be 9.6–11.1 times of the smooth duct.

Karwa and Maheshwari [66] carried out experimental study of heat transfer and friction in a rectangular section duct with transverse fully perforated baffles (open area ratio of 46.8%) as in Fig. 45 and half perforated baffles (open area ratio of 26%) affixed to one of the wall over the range of P/e: 7.2–28.8 & Re: 2700–11,150. Enhancement of 79–169% in Nusselt number was reported over the smooth duct for fully perforated baffles & 133–274% for the half perforated baffles while the friction factor for the fully perforated baffles is 2.98–8.02 times of that for smooth duct & is 4.42–17.5 times for the half perforated baffles.

Tabish Alam et al. [67] investigate the effect of circularity of perforation holes in V-shaped blockages on heat and friction factor characteristics of rectangular solar air heater duct. He created a hole on the V-shaped rib from circular to square shown in fig 46. With varying relative pitch of 4 to 12, relative blockage height of 0.4 to 1.0, open area ratio of 5% - 20% ,angle of attack 30-75^0 , also experiment has been done in Reynolds number between 2000 and 20,000.This absorber plate is expose to uniform heat flux . He found in non-circular perforation holes higher heat transfer as compare to circular hole and maximum heat transfer rate and friction factor is found at 60^0 as well as highest value of Nusselt number is found at pitch ratio P/e = 8, and f =4.

8. Conclusions

(1)Use of artificially roughened surfaces with different type of roughness geometries of different shapes, sizes and orientation is found to be the most effective technique to enhance the heat transfer rate with little penalty of friction.

(2) Roughness in the form of ribs, wire matrix and dimples were mainly suggested by different investigators to achieve better thermal performance. Among all, rib roughness was found the best performer as far as thermal performance is concerned.

(3) Transverse rib roughness enhances the heat transfer coefficient by flow separation and generation of vortices on the upstream and downstream of rib and reattachment of flow in the inter rib spaces[54].

(4) Angling of transverse rib further enhances the heat transfer on account of the movement of vortices along the rib and formation of a secondary flow cell which results in high heat flow region near the leading end. V-shaping of a long angled rib helps in the formation of two secondary flow cells as compared to one in case of an angled rib resulting in still higher heat transfer rate[54].

(5) Producing a gap in the inclined rib is found to enhance the heat transfer by breaking the secondary flow and producing higher level of turbulence in the fluid downstream of the rib. A similar gap in both the limbs of V-rib further enhances the heat transfer by introducing similar effects in both the limbs. Further the use of multi v-rib is found to enhance the heat transfer by increasing the number of secondary flow cells several times[54].

(6) In general, Nusselt number increases whereas the friction factor decreases with an increase of (Re). The values of Nu & friction factor are substantially higher as compared to those obtained for smooth plates. This is due to distinct change in the fluid flow characteristics as a result of roughness that causes flow separations, reattachments & generation of secondary flows.[31]

(7) It was observed that the rate of increase of Nusselt number with an increase in Reynolds number is lower than the rate of increase of friction factor; this appears due to the fact that at relatively higher values of relative roughness height, the re-attachment of free shear layer might not occur and the rate of heat transfer enhancement will not be proportional to that of friction factor.[31]

(8) As far as different rib geometries in experiments studied so far, the protrusions or dimple shape elements offers minimum friction factor value when compared to increase in the Nusselt number value at the optimum value of parameters selected than other rib elements.

(9) Studies have been reported with high roughness height generally called baffles and they show high rate of heat transfer but baffle blockage increase the pressure drop which

is a serious concern thus investigators must look to reduce the pressure drop which can attained by Perforation.

(10)It is found in the literature that perforated blocks/baffles are thermo-hydraulically better in comparison to solid blocks/ baffles because perforation in blocks/baffles enhances the Nusselt number due to elimination of hot spot just behind the ribs.

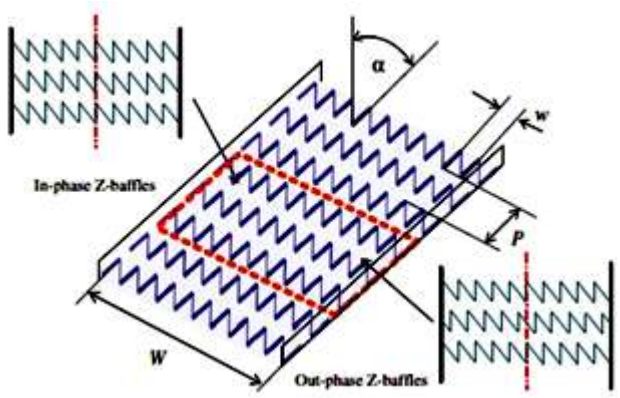

Fig.43. Z shaped baffles

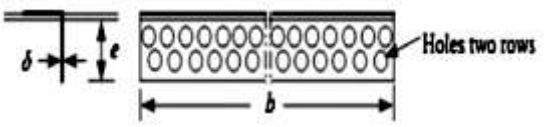

Fig.44 Transverse perforated baffles with two rows

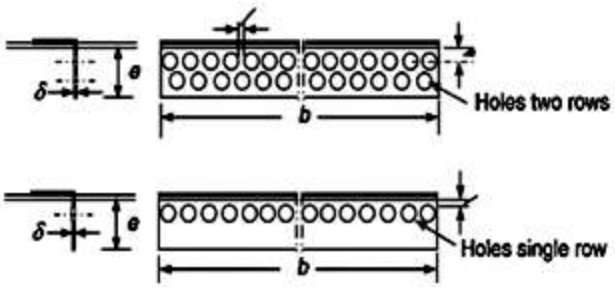

Fig.45 Transverse perforated baffles with double & single row

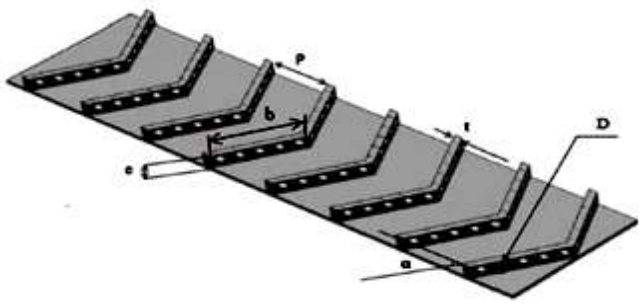

Fig.46 V shaped baffles with holes

References

[1] S. Chamoli , N.S. Thakur, J.S. Saini. A review of turbulence promoters used in solar thermal systems. Renewable and Sustainable Energy Reviews 16 (2012) 3154– 3175

[2] Duffie JA, Beckman WA. Solar engineering thermal processes. New York: John Wiley; 1991

[3] Varun, Saini RP, Singal SK. A review on roughness geometry used in solar air heaters. Solar Energy2007; 81:1340–50

[4] Bhatti MS, Shah RK. Turbulent and transition flow convective heat transfer in ducts. In: Kakac S, Shah RK, Aung W, editors. Hand book of single-phase convective heat transfer. New York: John Willey & Sons; 1987 [chapter 4].

[5] Patil AK, Saini JS, Kumar K. A comprehensive review on roughness geometries and investigation techniques used in artificially roughened solar air heaters. Int J Renewable Energy Res 2012;2(1).

[6] Karwa Rajendra, Chauhan Kalpana. Performance evaluation of solar air heaters having V-down discrete rib roughness on the absorber plate. Energy 2010;35:398–409.

[7] Prasad BN, Saini JS. Optimal thermo hydraulic performance of artificially roughened solar air heater. Sol Energy1991; 47:91–6.

[8] Prasad BN, Saini JS. Effect of artificial roughness on heat transfer and friction factor in a solar air heater. Sol Energy 1988; 41:555-60.

[9] Taslim ME, Li T, Kretcher DM. Experimental heat transfer and friction in channels roughened with angled, v-shaped and discrete ribs on two opposite walls. Trans ASME J Turbo mach 1996; 118:20–8.

[10] Aharwal KR, Gandhi BK, Saini JS. Experimental investigation on heat-transfer enhancement due to a gap in an inclined continuous rib arrangement in a rectangular duct of solar air heater. Renew Energy 2008;33:585-96

[11] Kumar Anil, Saini RP, Saini J S. Experimental investigation on heat transfer and fluid flow characteristics of air flow in a rectangular duct with Multi v-shaped rib with gap roughness on the heated plate 2012:1733–49.

[12] Muluwork KB. Investigations on fluid flow and heat transfer in roughened absorber solar heaters [Ph.D. dissertation]. IIT,Roorkee-247667,India;2000

[13] Sparrow EM, Hossfeld LM. Effect of rounding of protruding edges on heat transfer and pressure drop in a duct. Int J Heat Mass Transfer 1984; 27: 1715–23.

[14] Karwa R, Solanki SC, Saini JS. Heat transfer coefficient and friction factor Correlations for the transitional flow regime in rib roughened rectangular ducts, vol.42;1999.p.1597–1615.

[15] Han JC, Park JS. Developing heat transfer in rectangular channels with rib turbulators. Int J Heat MassTransf 1988; 31:183–95.

[16] Yeh Ho-Ming, LinChi-Yen. The effect of collector aspect ratio on the collector efficiency of upward-type flat-plate solar air heaters. Energy1996; 21:843–50.

[17] Han JC, Glicksman LR, Rohsenow WM. An investigation of heat transfer and friction for rib roughened surfaces. Int J Heat MassTransf 1978; 21:1143–56.

[18] Bhargava AK, Rizzi G. A solar air heater with variable flow passage width. Energy Convers Manag1990; 30:329–32.

[19] Hegazy Adel A. Optimization of flow channel depth for conventional flat-plate solar air heaters. Renew Energy 1996; 7:15–21.

[20] Kays WB. Convective heat and mass transfer. New York: McGraw Hill Book Co.; 1966. p. 197–8.

[21] Prasad K, Mullick SC. Heat transfer characteristics of a solar air heater used for drying purposes. Appl Energy 1983; 13:83–93.

[22] Gupta D, Solanki SC, Saini JS. Heat and fluid flow in rectangular solar air heater ducts having transverse rib roughness on absorber plates. Sol Energy 1993; 51:31–7.

[23] Verma SK, Prasad BN. Investigation for the optimal thermo hydraulic performance of artificially roughened solar air heaters. Renew Energy 2000; 20:19–36.

[24] Sahu MM, Bhagoria JL. Augmentation of heat transfer coefficient by using 90^0 broken transverse ribs on absorber plate of solar air heater. Renew Energy 2005; 30:2057–63.

[25] Han JC, Park CK. Augmented heat transfer in rectangular channels of narrow aspect ratios with rib turbulators. Int J Heat Mass Tran 1989; 32:1619-30.

[26] Gupta D, Solanki SC, Saini JS. Thermo hydraulic performance of solar air heaters with roughened absorber plates. Solar Energy 1997; 61:33–42.

[27] Lu B, Jiang PX. Experimental and numerical investigation of convection heat transfer in a rectangular channel with angled ribs. Exp Therm Fluid Sci 2006; 30:513-21.

[28] Aharwal KR, Gandhi BK, Saini JS. Experimental investigation on heat-transfer enhance-ment due to a gap in an inclined continuous rib arrangement in a rectangular duct of solar air heater. Renew Energy 2008; 33:585–96.

[29] Kumar ST, Mittal V, Thakur NS, Kumar A. Heat transfer and friction factor correlations for rectangular solar air heater duct having 60^0 inclined continuous discrete rib arrangement. Br J Appl Sci Technol 2011; 3:67-93.

[30] Varun, Saini RP, Singal SK. Investigation of thermal performance of solar air heater having roughness elements as a combination of inclined and transverse ribs on absorber plate. Renew Energy 2008; l33:1398–405.

[31] Momin AME, Saini JS, Solanki SC. Heat transfer and friction in solar air heater duct with v-shaped rib roughness on absorber plate. Int J Heat Mass Transfer 2002; 45:3383–96.

[32] Singh Sukhmeet, Chander S, Saini JS. Heat transfer and friction factor correlations of solar air heater ducts artificially roughened with discrete V-down ribs. Energy 2011; 36:5053–64.

[33] Sukhmeet S, Chandar S, Saini JS. Investigations on thermo-hydraulic performance due to flow-attack-angle in V-down rib with gap in a rectangular duct of solar air heater. Appl Energy 2012; 97:907-12.

[34] Karwa RK. Experimental studies of augmented heat transfer and friction in asymmetrically heated rectangular ducts with ribs on heated wall in transverse, inclined, v-continuous and v-discrete pattern. Int Commun Heat Mass Transfer 2003; 30:241–50.

[35] Hans VS, Saini RP, Saini JS. Heat transfer and friction factor correlations for a solar air heater duct roughened artificially with multiple V-ribs. Sol Energy 2010; 84:898–911.

[36] Lanjewar A, Bhagoria JL, Sarviya RM. Heat transfer and friction in solar air heater duct with W-shaped rib roughness on absorber plate. Energy 2011; 36: 4531-41

[37] Lanjewar A, Bhagoria JL, Sarviya RM. Experimental study of augmented heat transfer and friction in solar air heater with different orientations of W-Rib roughness. Exp Therm Fluid Sci 2011; 35:986–95.

[38] Kumar A, Bhagoria JL, Sarviya RM. International 19th national & 8th ISHMT- ASME heat and mass transfer conference heat transfer enhancement in channel of solar air collect or by using discrete W-shaped artificial roughened absorber; 2008.

[39] Kumar A, Bhagoria JL, Sarviya RM. Heat transfer and friction correlations for artificially roughened solar air heater duct with discrete W-shaped ribs. Energy Convers Manage 2009; 50:2106-17.

[40] Saini SK, Saini RP. Development of correlations for Nusselt number and friction factor for solar air heater with roughened duct having arc-shaped wire as artificial roughness. Solar Energy 2008; 82:1118–30.

[41] V.S. Hans, R.S. Gill, Sukhmeet Singh. Heat transfer & friction factor correlations for a solar air heater duct roughened artificially with broken arc ribs. Experimental Thermal and Fluid Science 80 (2017) 77–89.

[42] R S Gill, V S Hans, J S Saini. Heat Transfer and Friction Characteristics of Solar Air Heater duct Roughened by Broken Arc Shaped Ribs Combined with Staggered Rib Piece. IJERT ISSN: 2278-0181,Vol. 4 Issue 11, November-2015.

[43] Anil P. Singh, Varun, Siddhartha. Heat transfer and friction factor correlations for multiple arc shape roughness elements on the absorber plate used in solar air heaters. Experimental Thermal and Fluid Science 54 (2014) 117–126.

[44] N.K. Pandey, V.K. Bajpai, Varun. Experimental investigation of heat transfer augmentation using multiple arcs with gap on absorber plate of solar air heater. Solar Energy 134 (2016) 314–326.

[45] Jaurker AR, Saini JS, Gandhi BK. Heat transfer and friction characteristics of rectangular solar air heater duct using rib-grooved artificial roughness. Solar Energy 2006; 80:895–7.

[46] Layek A, Saini JS, Solanki SC. Second law optimization of a solar air heater having chamfered rib-groove roughness on absorber plate. Renew Energy 2007; 32:1967–80.

[47] Saini RP, Saini JS. Heat transfer & friction factor correlations for artificially roughened ducts with expanded metal mesh as roughness element. Int J Heat Mass Transf 1995; 40:973–986.

[48] Bhagoria JL, Saini JS, Solanki SC. Heat transfer coefficient and friction factor correlations for rectangular solar air heater duct having transverse wedge shaped rib roughness on the absorber plate. Renew Energy 2002; 25:341–69.

[49] Karmare SV, Tikekar AN. Heat transfer and friction factor correlation for artificially roughened duct with metal grit ribs. Int J Heat Mass Transfer 2007; 50:4342–51.

[50] Saini RP, Verma J. Heat transfer and friction factor correlations for a duct having dimple-shaped artificial roughness for solar air heaters. Energy 2008; l33:1277–87.

[51] Bhusan Brij, Singh Ranjit. Thermal and thermo hydraulic performance of roughened solar air heater having protruded absorber plate. Sol Energy 2012; 86:3388–96.

[52] Sanjay Yadav, Maneesh Kaushal, Siddhartha Varun. Nusselt number and friction factor correlations for solar air heater duct having protrusions as roughness elements on absorber plate. Exp Therm Fluid Sci 2013; 44:34–41.

[53] Sethi Muneesh, Varun Thakur NS. Correlations for solar air heater duct with dimpled shape roughness elements on absorber plate. Sol Energy.2012; 86: 2852–61.

[54] Anil Kumar, R.P. Saini , J.S. Saini. Heat and fluid flow characteristics of roughened solar air heater ducts e A review. Renewable Energy 47 (2012) 77-94

[55] Kumar A, Saini RP, Saini JS. Heat transfer and friction factor of solar air heater having duct roughened artificially with discrete multiple V-ribs. J Renew Sustain Energy 2012; 4:033103

[56] Duffie JA, Beckman WA. Solar engineering of thermal processes. New York: Wiley; 1980.

[57] Frank K, Mark SB. Principles of heat transfer. Colorado: Thomson Learning Inc.; 2001.

[58] Webb RL, Eckort ERG, Goldstein KJ. Heat transfer & friction in tubes with repeated rib roughness. Int J Heat Mass Transf 1971;14:601–17.

[59] Lewis MJ. Optimizing the thermo hydraulic performance of rough surfaces. Int J Heat Mass Transf 1975;181243-8 1975;18.

[60] Sunil Chamoli, N.S. Thakur, J.S. Saini. A review of turbulence promoters used in solar thermal systems. Renewable and Sustainable Energy Reviews 16 (2012) 3154– 3175

[61] Yeh HM, Chou WH. Efficiency of solar air heaters with baffles. Energy 1991;16:983–7.

[62] Bopche SB, Tandale MS. Experimental investigation on heat transfer and frictional characteristics of a turbulator roughened solar air heater duct. Int J Heat Mass Transfer 2009;52:2834–48.

[63] Promvonge P. Heat transfer and pressure drop in a channel with multiple 60◦ V baffles. Int Commun Heat Mass Transfer 2010;37:835–40.

[64] Sriromreun P, Thianpong C, Promvonge P. Experimental and numerical study on heat transfer enhancement in a channel with Z-shaped baffles. Int Commun HeatMassTransf2012;39:945–52.

[65] Karwa R, Maheshwari BK, Karwa N. Int Commun Heat Mass Transfer 2005;32:275–84.

[66] Karwa R, Maheshwari BK. Heat transfer and friction in an asymmetrically heated rectangular duct with half and fully perforated baffles at different pitches. Int Commun Heat Mass Transf 2009;36:264–8.

[67] Alam Tabish et al.,"Effect of circularity of perforation holes in V-shaped blockages on heat transfer and friction characteristics of rectangular solar air heater duct," Energy Conversion and Management , vol. 86, pp. 952–963, 2014.

[68] M.K. Gupta, S.C. Kaushik. Performance evaluation of solar air heater for various artificial roughness geometries based on energy, effective and exergy efficiencies. Renewable Energy 34 (2009) 465–476.